

**APPLIED ELECTROCHEMISTRY
AND METAL CORROSION PROTECTION**

**Synthesis and Electrochemical Performance of the Li-Rich
Cathode Material $\text{Li}_{1.17}\text{Ni}_{0.12}\text{Co}_{0.13}\text{Mn}_{0.58}\text{O}_2$
for Lithium-Ion Batteries**

A. A. Popovich^a, M. Yu. Maximov^a, A. O. Silin^a, P. A. Novikov^{a*},
Yu. M. Koshtyai^b, and A. M. Rumyantsev^b

^a Peter the Great St. Petersburg Polytechnic University, Russia

^b Ioffe Physical-Technical Institute, Russian Academy of Sciences, St. Petersburg, Russia

*e-mail: novikov.p.a@gmail.com

Received September 28, 2016

Abstract—Lithium-riched cathode material for lithium-ion batteries, $\text{Li}_{1.17}\text{Ni}_{0.12}\text{Co}_{0.13}\text{Mn}_{0.58}\text{O}_2$, was synthesized via crystallization from a solution of metal acetates, followed by a thermal treatment of the material obtained as a powder. The phase, elemental, and granulometric compositions of the material were examined, as well as the morphology of the powder particles obtained. The discharge capacity of the material in relation to the charging voltage was found from the results of electrochemical tests, and endurance tests were performed. The discharge capacity upon 85 charge/discharge cycles at voltages in the range 2.8–4.8 and a current of 0.1C was about 180 mA h g^{-1} .

DOI: 10.1134/S1070427216100074

Raising the specific energy of lithium-ion batteries (LIBs) is one of the main requirements of engineers involved in the development of portable electronics, electric (hybrid) vehicles, etc. LIBs based on cathode materials with high content of cobalt and(or) nickel are unsafe because of the release of a large amount of heat on their being short-circuited or mechanically damaged. Moreover, degradation occurs in prolonged operation of batteries with cathodes based on LiCoO_2 , which impairs their electrochemical characteristics and specific capacity, and this, in turn, forces present-day researchers to find and develop more perfect cathode materials.

The results of a study of an alternative lithium-riched cathode material for lithium-ion batteries were first reported in 2007. This is a nanocomposite consist of two phases distributed in the volume of the material: Li_2MnO_3 ($\text{Li}[\text{Li}_{1/3}\text{Mn}_{2/3}]\text{O}_2$) solid solution and LiMO_2 , where $\text{M} = \text{Ni}, \text{Co}, \text{Mn}$ [1]. Both these phases have a layered structure. The activation of the Li_2MnO_3 phase, owing to which the specific characteristics of the material are improved, occurs at potentials of 4.4 V and higher relative to metallic lithium. The distribution of Li_2MnO_3 within the bulk of the cathode material enables a reversible

intercalation/deintercalation of lithium in the material, with the cyclic stability of the cathode thereby improved [2–4]. Lithium-riched cathode materials have a specific discharge capacity of about 240 mA h g^{-1} at voltages in the range 2.0–4.8 V. For example, a specific discharge capacity of about 250 mA h g^{-1} have been detected for $\text{Li}_{1.2}\text{Ni}_{0.15}\text{Co}_{0.10}\text{Mn}_{0.55}\text{O}_2$ at potentials of 2.0–4.8 V [5–8]. The specific energy of LIBs depends, in particular, on the specific capacity and on the potential of the cathode material relative to the anode. The low content of cobalt and increased content of the less expensive manganese make lower the cost of the cathode material and, as a consequence, that of LIBs [9–13]. Owing to these advantages, the materials of this class attract increasing attention of scientists developing cathode materials and LIBs [1, 9].

The list of materials of this class is rather extensive and one of research areas in this field is the choice of a material with the optimal composition. In the present communication, we describe the synthesis of the previously unstudied material with formula $\text{Li}_{1.17}\text{Ni}_{0.12}\text{Co}_{0.13}\text{Mn}_{0.58}\text{O}_2$ and present the results of its analysis.

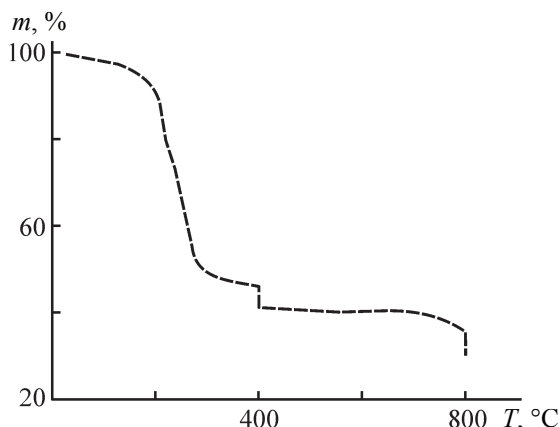


Fig. 1. TGA curve for thermal treatment of a mixture of metal acetates. (*m*) Mass and (*T*) temperature.

EXPERIMENTAL

Samples of the lithium-riched material $\text{Li}_{1.17}\text{Ni}_{0.12}\text{Co}_{0.13}\text{Mn}_{0.58}\text{O}_2$ were synthesized from a solution of metal acetates with pH 4, produced by dissolution of Li, Ni, and Mn salts in ethanol under permanent agitation with a magnetic stirrer at 40°C in the course of 40 min. The ethanolic solution containing Li, Ni, Co, and Mn acetates in the concentrations corresponding to the stoichiometric coefficients of the compound was dried in a vacuum at 100°C for 6 h until the solvent was completely evaporated. The resulting dark magenta mixture of metal acetates was subjected to a

thermal treatment in air. The thermal-treatment mode was determined by using the results of a thermogravimetric analysis (Fig. 1) and making an analysis of published data [1]: heating to 400°C at a rate of 10 deg min⁻¹, keeping at 400°C for 4 h, heating to 800°C at a rate of 10 deg min⁻¹, and keeping at 800°C for 6 h. Agglomerates of the thus synthesized cathode material were ground in ethanol in a Pulverisette 4 planetary mill at a 1 : 200 loading rate and rotation speed of 300 rpm for 3 h.

The phase and elemental compositions and the morphology of the powder were examined by X-ray diffraction analysis (XRD, Bruker D8 Discover), scanning electron microscopy (SEM), and Energy-dispersive X-ray spectroscopy (EDS) [Zeiss SUPRA 40VP with In-lens SE and SE2 secondary-electron detectors and four-quadrant detector of backscattered electrons (AsB)] at Resource centers “X-ray diffraction methods of study” and “Nanotechnologies” of the Scientific Park at St. Petersburg State University, respectively. The granulometric composition of the ground powder of the cathode material was determined in a gas medium with an Analysette 22 NanoTec laser particle-size analyzer (Fritsch).

The electrochemical studies were performed in CR2032 coin cells relative to lithium with BST8-MA battery analyzers (10 mA, MTI Corp.). To fabricate electrodes, an active paste based on *N*-methylpyrrolidone, cathode material ($\text{Li}_{1.17}\text{Ni}_{0.12}\text{Co}_{0.13}\text{Mn}_{0.58}\text{O}_2$), binder (polyvinylidene fluoride, Kynar 761A, Arkema), and

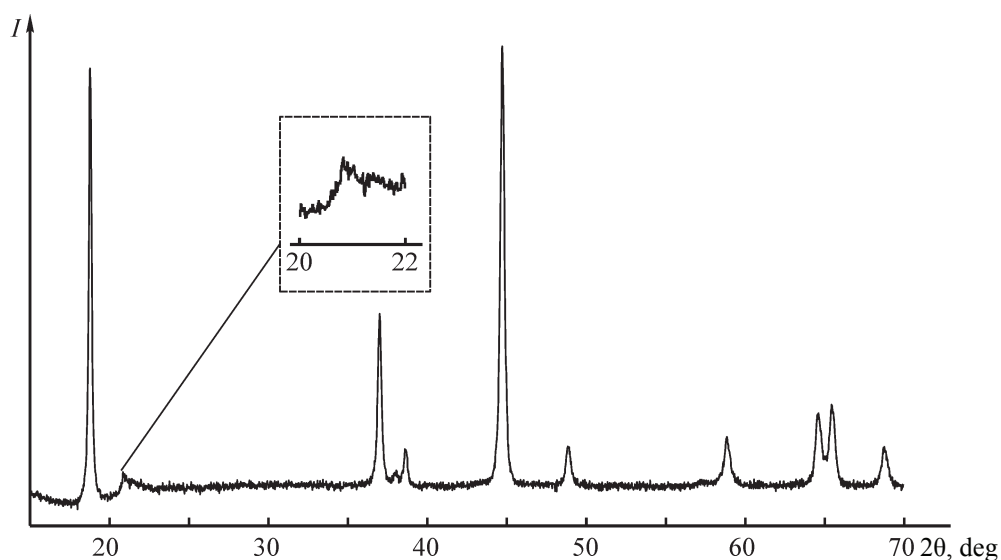


Fig. 2. Phase composition of the $\text{Li}_{1.17}\text{Ni}_{0.12}\text{Co}_{0.13}\text{Mn}_{0.58}\text{O}_2$ cathode material upon its thermal treatment. (*I*) Intensity and (2θ) Bragg angle.

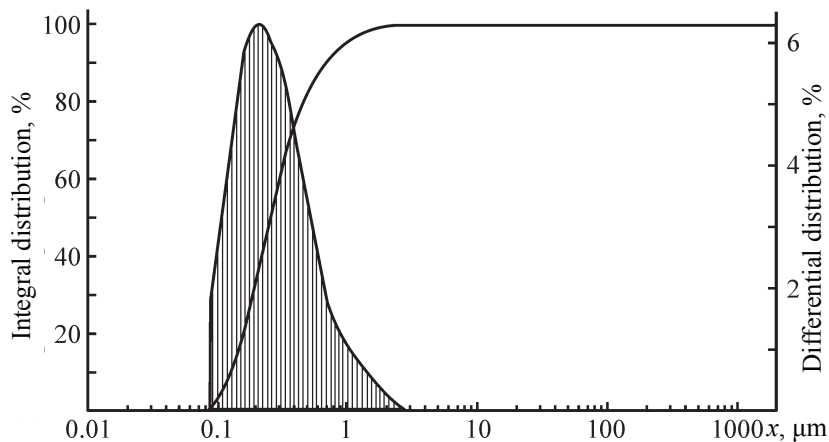


Fig. 3. Granulometric composition of the cathode material synthesized in the study. (x) Particle size.

carbon black (Super C65, Timcal) were deposited onto an aluminum foil in 80/10/10 mass ratio, respectively. As the anode, separator, and electrode served lithium foil, Celgard 2325, and TC-E918 (Tinci), respectively. The disk cases were assembled within a VGB6 glove box in the atmosphere of dry argon. To obtain a high specific capacity, we performed a step-by-step activation of the cathode material at 0.1C, the final charging voltage was (V): 4.4, 4 cycles; 4.6, 4 cycles; and 4.8, subsequent cycles [1]. The final discharge voltage was 2.8 V at 0.1C.

RESULTS AND DISCUSSION

Most of reflections in the diffraction pattern (Fig. 2) correspond to a layered hexagonal structure belonging to R3M space group characteristic of lithiated mixed nickel-cobalt-manganese oxides. A high-intensity peak at $2\theta = 19^\circ$, which corresponds to the <003> reflection plane, indicates that the material has structural features favorable for obtaining high electrochemical characteristics [6]. A peak indicating that the monoclinic structure ($C2/m$) of the $\text{Li}(\text{Li}_{1/3}\text{Mn}_{2/3})\text{O}_2$ phase is observed at $2\theta = 20-22^\circ$ [3, 6]. Thus, two phases, Li_2MnO_3 and LiMO_2 , are present in the structure of the material according to XPA data.

The powdered cathode material has agglomerates 10–100 μm in size. Prior to preparing the active paste, it was ground in a planetary mill. On being ground, the material had the following parameter of the particle size distribution (Fig. 3): D_{10} , 0.1 μm , D_{50} , 0.2 μm , D_{90} , 0.7 μm .

Because the device used to measure the particle size distribution has the lower particle-size limit of 100 nm, we performed a SEM study to determine whether finer

particles are present and to examine their morphology. Analysis of the SEM micrograph of the powder in Fig. 4 confirms the presence of a significant amount of particles smaller than 100 nm, with particles about 50 nm in size also observed. Most of particles have even faces indicative of the high degree of crystallization of the material, which is also confirmed by XRD data (Fig. 2).

According to the results of energy-dispersive spectroscopy, the material contains transition metals (nickel, cobalt, and manganese) in a ratio proportional to the stoichiometric coefficients in the formula.

Thus, the synthesis with vacuum-drying of salt solutions and subsequent thermal treatment yielded powders of the $\text{Li}_{1.17}\text{Ni}_{0.12}\text{Co}_{0.13}\text{Mn}_{0.58}\text{O}_2$ cathode material. Its phase composition corresponds to Li-rich cathode material [7]. According to the micrographs and

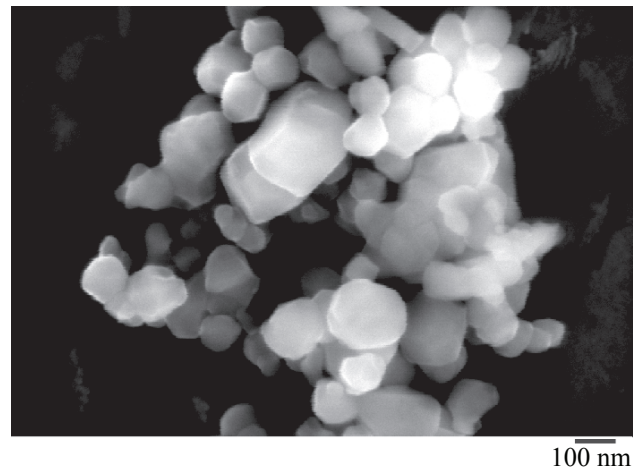


Fig. 4. SEM micrograph of the $\text{Li}_{1.17}\text{Ni}_{0.12}\text{Co}_{0.13}\text{Mn}_{0.58}\text{O}_2$ cathode material.

Relationship between the voltage and electrochemical processes [8]

Anodic processes relative to Li/Li ⁺ (charging)		Cathodic processes relative to Li/Li ⁺ (discharge)	
voltage, V	change of the oxidation state	voltage, V	change of the oxidation state
3.3	Mn ³⁺ Mn ⁴⁺	4.3	Co ³⁺ Co ⁴⁺
3.8	Ni ²⁺ Ni ⁴⁺	3.5	Ni ²⁺ Ni ⁴⁺
3.9 (4.0 in the first cycle)	Ni ²⁺ Ni ⁴⁺	2.9	Mn ³⁺ Mn ⁴⁺
4.4	Co ³⁺ Co ⁴⁺		
4.7 (in the first cycle)	O ²⁻ 0.5O ₂		

granulometric data, the average size of the resulting particles is about 100–200 μm.

It was shown in [7] that the specific capacity of the material grows with increasing charging voltage. In particular, processes promoting an improvement of the specific characteristics occur at different voltages (see table). However, a sharp increase in the charging voltage leads to a fast degradation of the material and to a decrease in its cyclic life, which may be due to the volumetric stresses in the lattice during the intercalation of lithium ions.

To reduce the volumetric stress in the lattice and thereby improve the cycling capacity and to obtain high specific capacities of the powder, it is necessary to perform a step-by-step activation of the material [5].

In the study, were activated the cathode material by the following scheme at a current density of 0.1C: 4 cycles at voltages of up to 4.4 V, 4 cycles up to 4.6 V, and subsequent cycles up to 4.8 V. The final discharge voltage was 2.8 V at 0.1C (Fig. 5a). As the charging

voltage was raised, the specific discharge capacity of the material increased: to 4.4 V, 80–85 mA h g⁻¹; to 4.6 V, 150–160 mA h g⁻¹, to 4.8 V, 190–210 mA h g⁻¹. In further cycling up to 4.8 V, the discharge capacity somewhat decreased after 15th cycle (Fig. 5b) to 175–180 mA h g⁻¹ and remained at this level during 85 cycles. The Coulomb efficiency varied within the range 90–95% in the activation stage of the material, being 98.5–99.5% after 15th cycle.

CONCLUSIONS

(1) Samples of a cathode material of composition $\text{Li}_{1.17}\text{Ni}_{0.12}\text{Co}_{0.13}\text{Mn}_{0.58}\text{O}_2$ were synthesized from metal acetates. According to the results of an X-ray phase analysis, the cathode material contains two layered crystalline phases ($\text{R}3\text{m}$ and $\text{C}2/\text{m}$ space groups) characteristic of lithium-riched mixed (Ni, Co, Mn) oxides.

(2) On being thermally treated, the powder of the cathode material of composition $\text{Li}_{1.17}\text{Ni}_{0.12}\text{Co}_{0.13}\text{Mn}_{0.58}\text{O}_2$

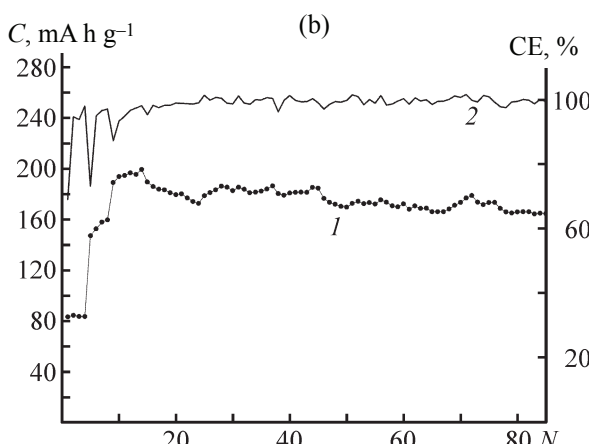
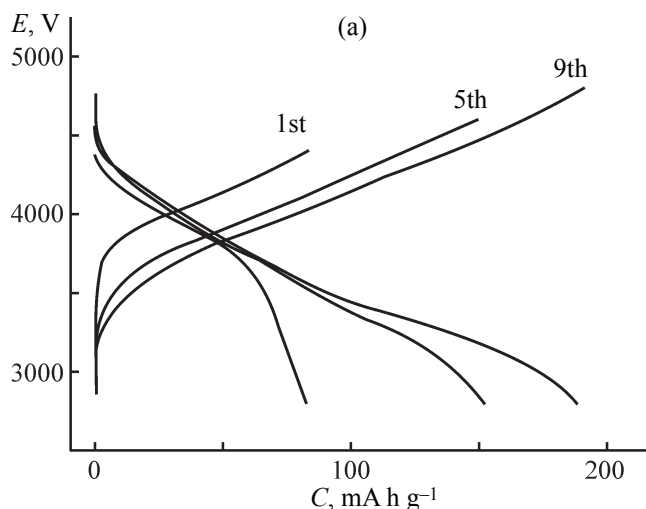


Fig. 5. (a) Variation of the specific capacity C on raising the charging voltage E (activation of the material) and (b) cycling stability of the $\text{Li}_{1.17}\text{Ni}_{0.12}\text{Co}_{0.13}\text{Mn}_{0.58}\text{O}_2$ cathode material. (N) Cycle number. (1) Cycling stability and (2) Coulomb efficiency CE.

is composed of agglomerates about 10–100 μm in size. According to granulometric data and scanning electron-microscopic images, the average particle size is 100–200 nm after the agglomerated segments are ground in a planetary mill.

(3) Electrochemical tests demonstrated that the specific discharge capacity of the $\text{Li}_{1.17}\text{Ni}_{0.12}\text{Co}_{0.13}\text{Mn}_{0.58}\text{O}_2$ material grows with increasing charging voltage: to 4.4 V, 80–85 mA h g⁻¹; to 4.6 V, 150–160 mA h g⁻¹, and to 4.8 V, 190–210 mA h g⁻¹. After the activation, the reversible discharge capacity varied within the range 175–180 mA h g⁻¹ during 85 charge/discharge (4.8–2.8) cycles.

ACKNOWLEDGMENTS

The study was financially supported by the Ministry of Education and Science of the Russian Federation, Agreement no. 14.584.21.0004 of 16.07.2014, unique identifier RFMEFI58414X0004.

REFERENCES

- Thackeray, M.M., Kang, S.H., Johnson, C.S., et al., *Mater. Chem.*, 2007, vol. 17, pp. 3112–3125.
- Yuan, X., Xu, Q., Wang, C., et al., *Power Sources*, 2015, vol. 279, p. 157.
- Karalee, A. Jarvis Zengqiang Deng, Lawrence F. Allard, et al., *Chem. Mater.*, 2011, vol. 23, no. 16, pp. 3614–3621.
- Park, S.H., Kang, S.H., Johnson, C.S., et al., *Electrochim. Commun.*, 2007, vol. 9, p. 262.
- Jin, X., Xu, Q., Liu, H., et al., *Electrochim. Acta*, 2014, vol. 136, p. 19.
- Cheng-chi Pan, Craig E. Banks, Wei-xin Song, et al., *Trans. Nonferrous Met. Soc. China*, 2013, vol. 23, pp. 108–119.
- Ying Bai, Yu Li, Chuan Wu, et al., *Energy Technol.*, 2015, vol. 3, pp. 843–850.
- Zheng, J.M., Wu, X.B., and Yang, Y., *Electrochim. Acta*, 2011, vol. 56, p. 3071.
- Lu, Z.H., MacNeil, D.D., and Dahn, J.R., *Electrochim. Solid-State Lett.*, 2001, vol. 4, pp. A191–A194.
- Ammundsen, B. and Paulsen, J., *Adv. Mater.*, 2001, vol. 13, pp. 943–956.
- Jiang, J., Eberman, K.W., Krause, L.J., and Dahn, J.R., *J. Electrochem. Soc.*, 2005, vol. 152, pp. A1879–A1889.
- Kang, S.H. and Amine, K., *J. Power Sources*, 2005, vol. 146, pp. 654–657.
- Lim, J.H., Bang, H., Lee, K.S., et al., *J. Power Sources*, 2009, vol. 189, pp. 571–575.